ELSEVIER

Journal of Luminescence 93 (2001) 107–114

JOURNAL OF LUMINESCENCE

www.elsevier.com/locate/jlumin

Luminescence and energy transfer in $CaAl_4O_7:Tb^{3+}$, Ce^{3+}

Dongdong Jia[a,b,*], Jing Zhu[a], Boqun Wu[b], S. E[c]

[a] *School of Materials Science & Engineering, Tsinghua University, Beijing 100084, People's Republic of China*
[b] *Central Iron and Steel Research Institute, Beijing 100081, People's Republic of China*
[c] *Changchun Institute of Physics, CAS, Chaqngchun,133001, Jilin, People's Republic of China*

Received 24 February 2000; received in revised form 1 November 2000; accepted 7 December 2000

Abstract

Samples of $CaAl_4O_7$ doped with Tb^{3+}, Ce^{3+}, and Tb^{3+} and Ce^{3+}, respectively are prepared by sintering. Microstructures are analyzed by X-ray diffraction and high-resolution transmission electron microscope experiments. The samples show single monoclinic phase. The blue Ce^{3+} emission at 440 nm is efficiently quenched in the sample of $CaAl_4O_7:Tb^{3+}$, Ce^{3+}, in which the dominant emission is in the green at 545 nm, originating from the transition of $^5D_4$ to $^7F_5$. Excitation spectrum of the $CaAl_4O_7:Tb^{3+}$, Ce^{3+}, monitoring at 545 nm of the green emission, consists of both contributions from Ce^{3+} and Tb^{3+}. 95% of total energy of Tb^{3+} green emission is transferred from Ce^{3+}.

Keywords: Photoluminescence; Energy transfer; Sensitization; $CaAl_4O_7:Tb^{3+}/Ce^{3+}$

1. Introduction

In searching of new phosphorous materials for emissive displays, selection of host materials is an essential issue. For example, the ligand field of hosts may modify the colors of the emissions of the activators [1,2]. The emission spectra of rare earth ions almost remain the same in different hosts, but the luminescent efficiency, chemical stability and durability largely depend on the physical properties of the hosts selected.

Comparing with the alkali earth sulfides [3,4] widely used for phosphor hosts in the past, alkaline earth aluminates are chemically stable in ambient environment, and are used as host materials in recent years. $CaAl_4O_7$ is selected as a host material in this work. It has monoclinic structure with $a = 1.289$ nm, $b = 0.889$ nm, $c = 0.544$ nm and $\beta = 106.93^\circ$ [5,6]. The lower symmetry without inversion may be good for higher parity allowed transition. Lasing emission has been reported in $Nd:CaAl_4O_7$ [7].

The Tb^{3+} and Ce^{3+} ions are two important rare earth ions, which have been used to produce green and blue emission [8]. In addition, Ce^{3+} is an efficient sensitizer to Tb^{3+}, which has been extensively studied [9].

In this work, Tb^{3+} or Ce^{3+} doped and Tb^{3+}/Ce^{3+} codoped $CaAl_4O_7$ phosphors are prepared. Photoluminescence and excitation spectra are investigated. Energy transfer from Ce^{3+} to Tb^{3+} is discussed.

*Correspondence address. School of Materials Science & Engineering, Tsinghua University, Beijing 100084, People's Republic of China. Tel.: +86-10-627-730-15; fax: +86-106-277-2507.

E-mail address: jiadong@public3.bta.net.cn (D. Jia).

0022-2313/01/$ - see front matter
PII: S0022-2313(01)00182-X

2. Experimental

The samples are prepared by sintering. Raw materials of $CaCO_3$, Al_2O_3, Tb_2O_3 and/or Ce_2O_3 are mixed according to the following formulas:

$$CaCO_3 + 2Al_2O_3 + 0.005Ce_2O_3 \rightarrow CaAl_4O_7 : 0.01Ce^{3+} + CO_2\uparrow,$$

$$CaCO_3 + 2Al_2O_3 + 0.005Tb_2O_3 \rightarrow CaAl_4O_7 : 0.01Tb^{3+} + CO_2\uparrow,$$

$$CaCO_3 + 2Al_2O_3 + 0.005Ce_2O_3 + 0.005Tb_2O_3 \rightarrow CaAl_4O_7 : 0.01Tb^{3+}, 0.01Ce^{3+} + CO_2\uparrow .$$

The samples are sintered under reduction condition ($N_2 + 5\%$ H_2). Sintering in oxidizing atmosphere (air), most of Ce^{3+} and Tb^{3+} will be oxidized both to Ce^{4+} and Tb^{4+} states and luminescence of the samples become very weak.

X-ray diffraction and high-resolution transmission electron microscope (HRTEM) experiments are carried out to analyze the structure of the samples. Excitation and emission spectra are studied.

3. Results and discussions

3.1. Structure of the sample host

X-ray diffraction spectra of the samples sintered in air and $N_2 + 5\%$ H_2 are obtained and shown in Fig. 1a and b, respectively. The results show that samples have $CaAl_4O_7$ monoclinic structure. Comparing the two X-ray diffraction patterns, the structures of the samples sintered in air and in $N_2 + 5\%$ H_2 reductive gas flow, do not have any difference so that sintering environment will not influence the structure of the host, but it will decide the valence states of the doped ions.

There are some very weak B_2O_3 peaks in the X-ray patterns, which may indicate the existence of B_2O_3. The HRTEM image of the $CaAl_4O_7:Tb^{3+}$, Ce^{3+} sample sintered in $N_2 + 5\%$ H_2, is shown in Fig. 2a and b. Fig. 2b is the diffraction pattern of Fig. 2a. In Fig. 2a, the sample lattice is very regular. No obvious defect is observed in the

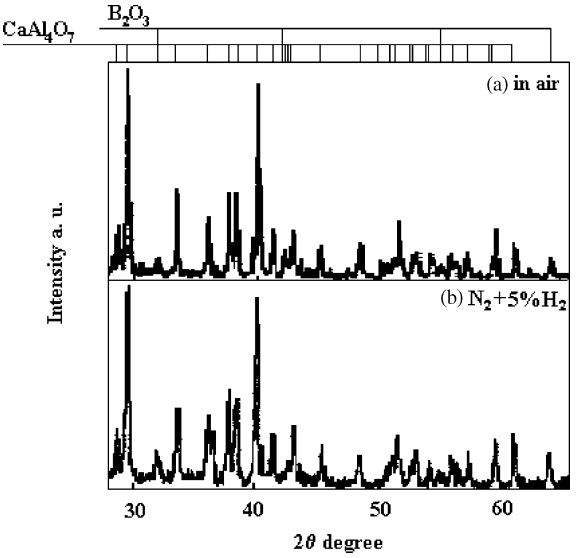

Fig. 1. X-ray diffraction spectra of $CaAl_4O_7:Tb^{3+}$, Ce^{3+}; (a) in air; (b) in $N_2 + 5\%$ H_2.

HRTEM image. Thus the quality of the $CaAl_4O_7:Tb^{3+}$, Ce^{3+} sample is quite good. From the results of HRTEM and X-ray diffraction, B_2O_3 is reasonably presumed that they do not go into the $CaAl_4O_7$ host and form $CaAl_{4-x}B_xO_7$. If there is any B^{3+} in the host, then some clear lattice distortions due to the difference of ion radii between B^{3+} and Al^{3+}, should be observed by normally assuming that B^{3+} should occupy Al^{3+} site in the host [10]. The B_2O_3 remains outside the $CaAl_4O_7$ grains during cooling process because of its lower melting temperature. Fig. 3a is the lattice structure of the $CaAl_4O_7:Tb^{3+}$, Ce^{3+} sample drawn by theoretical calculation and Fig. 3b is the diffraction pattern calculated. The trivalent Ce^{3+} and Tb^{3+} are also presumed to replace Ca^{2+} ions without going into the Al^{3+} sites too. This is because the room for Al^{3+} in $CaAl_4O_7$ is smaller than in $SrAl_2O_4$.

3.2. Photoluminescence and excitation spectra

Emission and excitation spectra of the $CaAl_4O_7:Ce^{3+}$ are shown in Fig. 4a and b, respectively. The emission of Ce^{3+} usually includes two bands of the transitions of 5d-excited state to

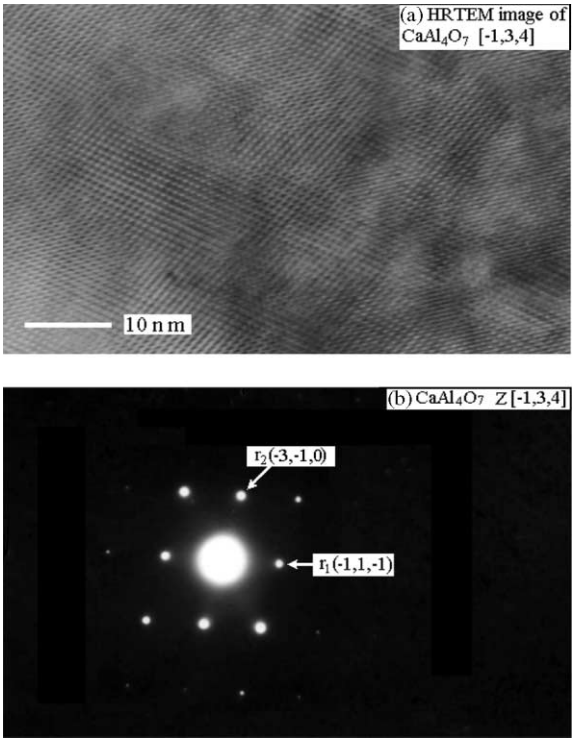

Fig. 2. High resolution transmission electron microscope (HRTEM) image of $CaAl_4O_7:Tb^{3+}$, Ce^{3+}. (a) HRTEM image of (−1, 3, 4) plane; (b) diffraction pattern of (a).

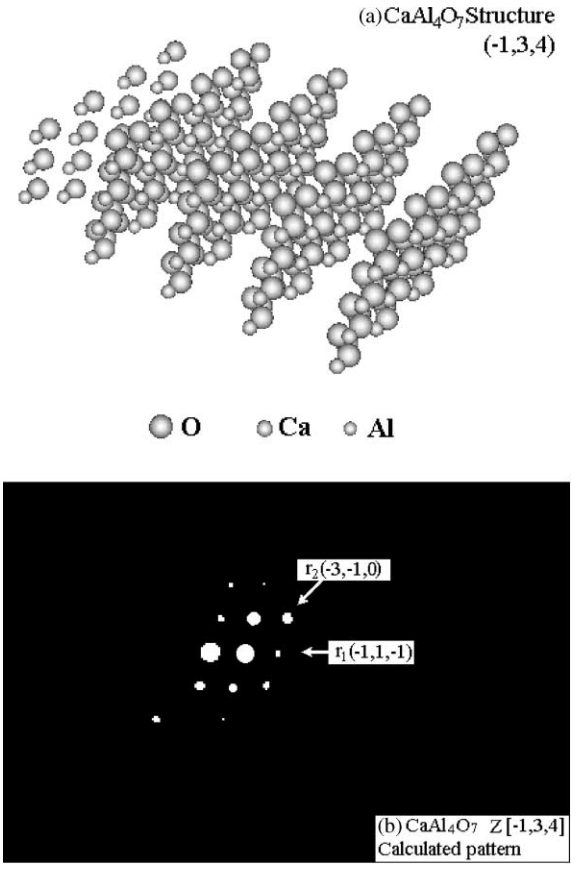

Fig. 3. (a) Calculated structure of $CaAl_4O_7$ view of (−1, 3, 4) plane; (b) calculated diffraction pattern of (a).

$^2F_{7/2}$ and $^2F_{5/2}$ states. The emission spectrum observed in $CaAl_4O_7:Ce^{3+}$ seems to consist of two of them in a single band, peaking at 440 nm. Its excitation peaks are found at 270, 307 and 357 nm in Fig. 4b, which correspond to the transitions from ground state of Ce^{3+} to its field splitting levels of $5d^1$ states [11].

The emission spectra of $CaAl_4O_7:Tb^{3+}$ and $CaAl_4O_7:Tb^{3+}$, Ce^{3+} are shown in Fig. 5a and b. The Tb^{3+} emission peaks are found at 485, 545, 590, 620, 660 and 690 nm, which are assigned to the $^5D_4$ to ^7F_J ($J=6$, 5, 4, 3, 2, 1) transitions of singly doped Tb^{3+} in $CaAl_4O_7$ (Fig. 5a). Some weak emissions from $^5D_3$ to ^7F_J ($J=5$, 4, 3, 2, 1, 0) are also found from 400 to 485 nm in Tb^{3+} singly doped sample [12]. The energy difference between $^5D_3$ and $^5D_4$ is the same as that between $^7F_0$ to $^7F_6$, which sometimes correspond to the energy transfer of identical centers, $^5D_3(Tb^{3+}) + {}^7F_6(Tb^{3+}) - {}^5D_4(Tb^{3+}) + {}^7F_0(Tb^{3+})$So that the $^5D_3$ to ^7F_J transitions of some high Tb^{3+}concentration materials are quenched by the energy transfer process mentioned above and thus only $^5D_4$ to ^7F_J emissions can be observed.

The emission intensity of Tb^{3+} in $CaAl_4O_7:Tb^{3+}$, Ce^{3+} (Fig. 5a) is stronger than that of Tb^{3+} in $CaAl_4O_7:Tb^{3+}$ (Fig. 5b) shows the result of Ce^{3+} to Tb^{3+} energy transfer. The $^5D_3$ to ^7F_J transitions of Tb^{3+} disappeared in Fig. 5b, and this is very much likely because of the energy transfer process taken place in the region from 400 to 500 nm [13].

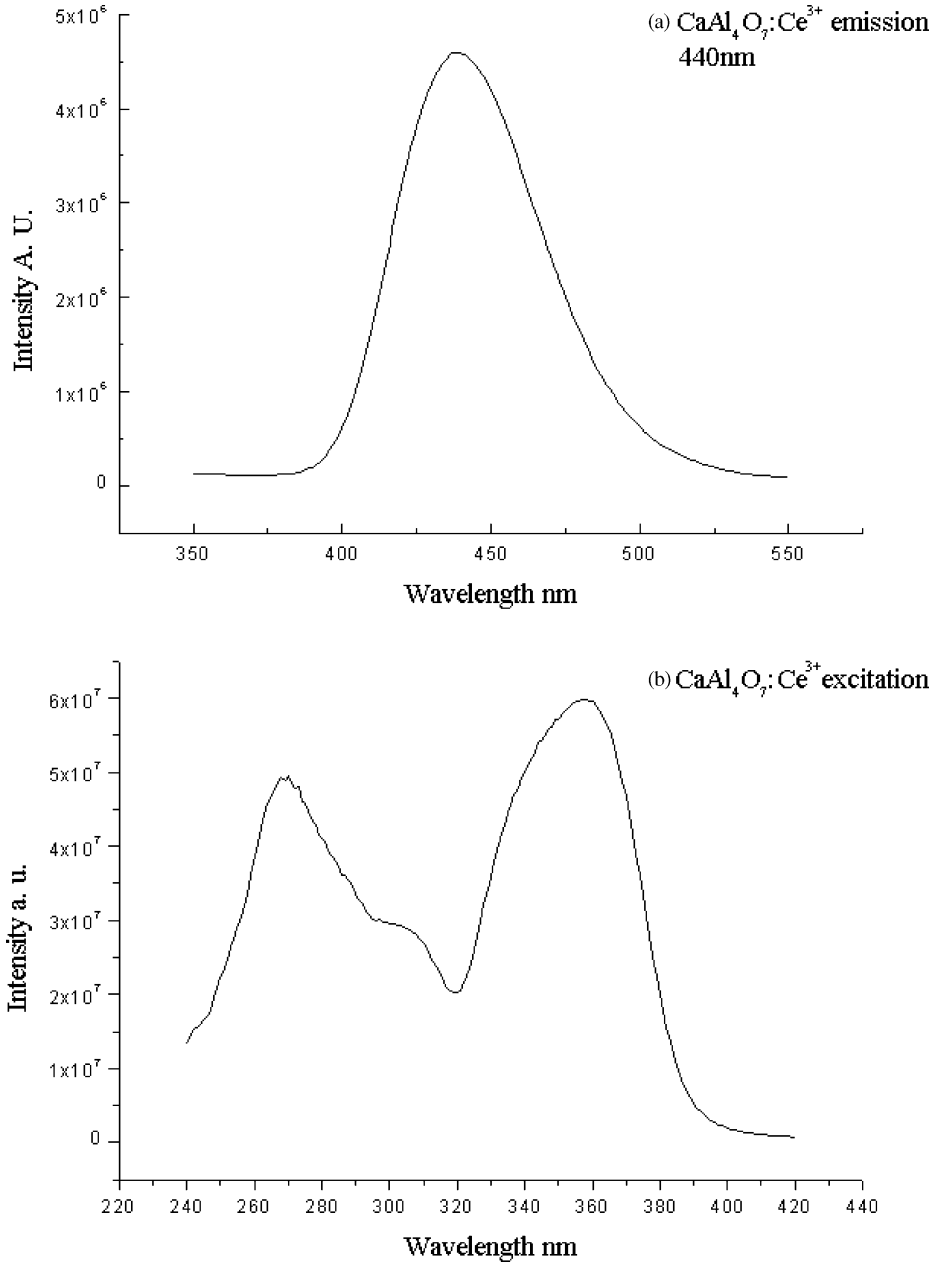

Fig. 4. Emission and excitation spectra of $CaAl_4O_7:Ce^{3+}$. (a) 5d–$^7F_{5/2,7/2}$ emission, peak at 440 nm; (b) 4f–5d excitations, peak at 270, 307 and 357 nm.

The excitation spectrum of the Tb^{3+} singly doped sample at $\lambda_{em}= 545$ nm, is shown in Fig. 6a. The excitation peaks are found to be strong at 283 nm and some weaker peaks at lower energies. The strong 283 nm peak is related to the f–d excitation of the Tb^{3+}, and the other peaks are the f–f excitations. Comparing the excitation spectra of the $CaAl_4O_7:Ce^{3+}$, $CaAl_4O_7:Tb^{3+}$

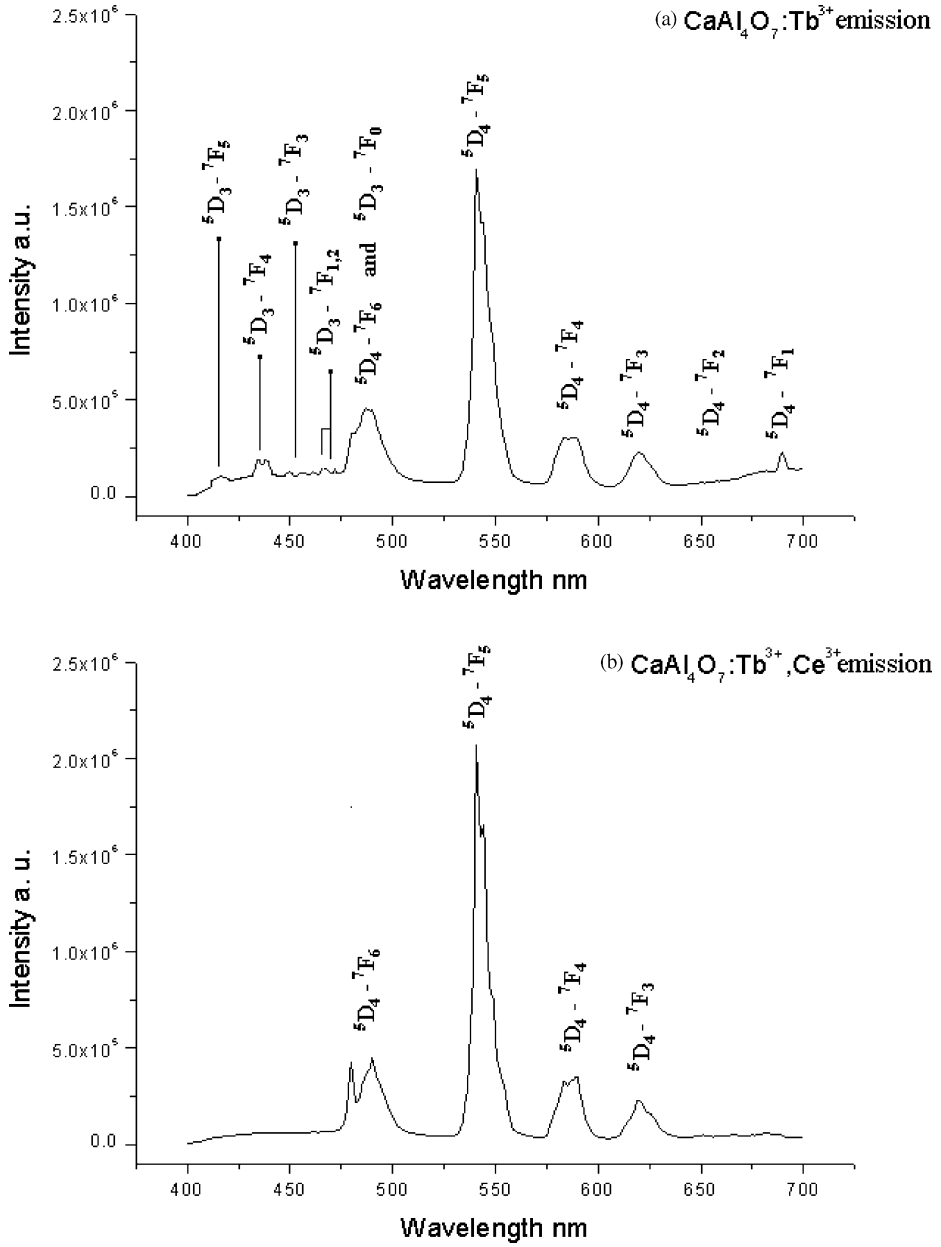

Fig. 5. Emission spectra of $CaAl_4O_7:Tb^{3+}$ and $CaAl_4O_7:Tb^{3+}$, Ce^{3+}. (a) $CaAl_4O_7:Tb^{3+}$ emission, ($^5D_3$,$^5D_4$–^7F_J); (b) $CaAl_4O_7:Tb^{3+}$, Ce^{3+} emission, ($^5D_4$–^7F_J). And $^5D_3$–^7F_J vanished.

and $CaAl_4O_7:Tb^{3+}$, Ce^{3+} samples in the 250–400 nm region, shown in Figs. 4b, 6a and b, one can find the energy transfer from Ce^{3+} emission to Tb^{3+} excitation because the excitation spectrum of $CaAl_4O_7:Tb^{3+}$, Ce^{3+} sample contains the Ce^{3+} excitations (Fig. 6b). The result calculated from the three normalized excitation spectra (Fig. 4b and Fig. 6a and b) shows that emission

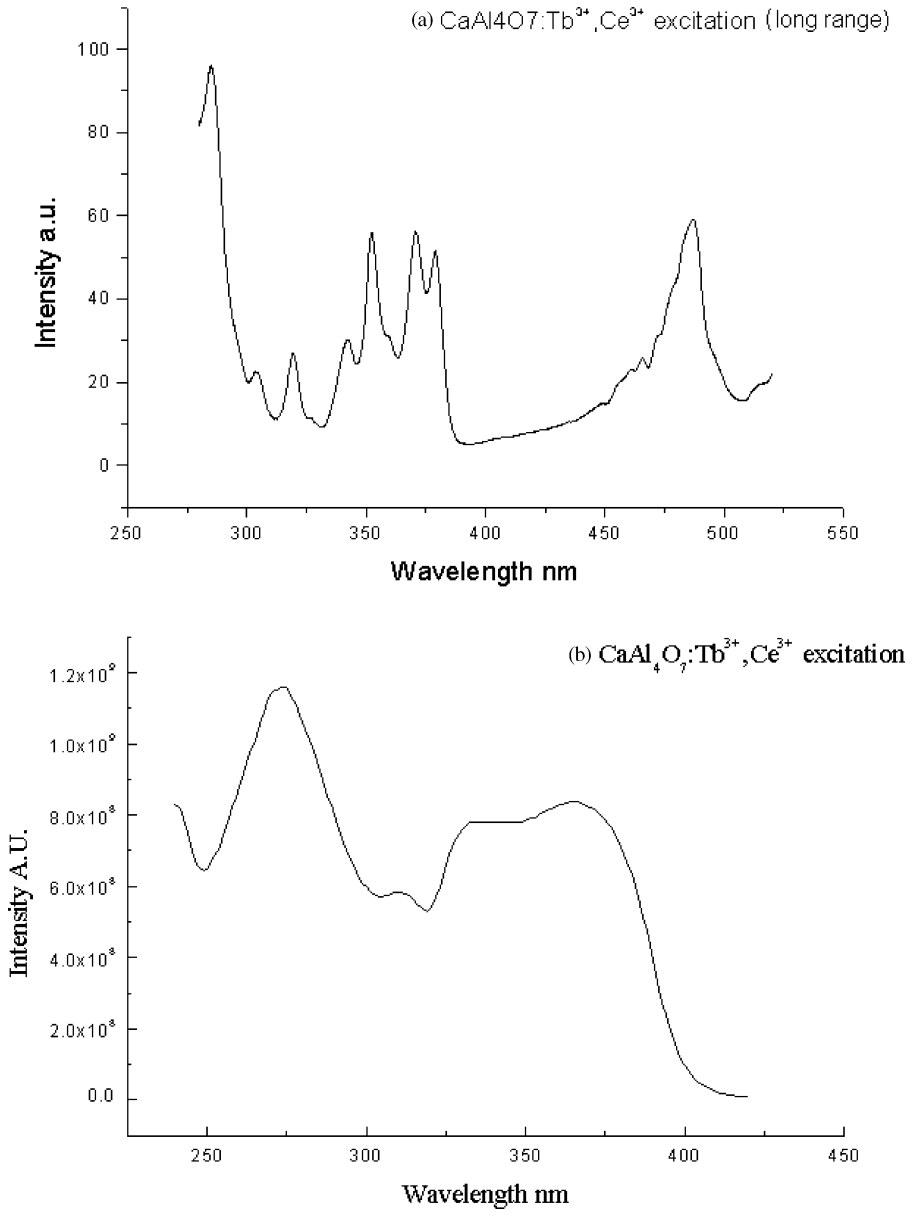

Fig. 6. Excitation spectra of samples showing energy transfer. (a) $CaAl_4O_7:Tb^{3+}$; (b) $CaAl_4O_7:Tb^{3+}$, Ce^{3+} (95% of Ce^{3+} and 5% of Tb^{3+}).

of Tb^{3+} in the $CaAl_4O_7:Tb^{3+}$, Ce^{3+} sample, at $\lambda_{em} = 545$ nm, contains about 95% contribution from the Ce^{3+} energy transfer and the other 5% is from the direct Tb^{3+} excitation. This result shows that Ce absorption in the Tb–Ce system is much stronger than that of Tb, because it is a spin and dipole allowed transition. Therefore the energy transfer from Ce to Tb or Ce sensitization effect dominates the energy process.

3.3. Energy transfer from Ce^{3+} to Tb^{3+}

The energy transfer process was first considered theoretically by Förster in 1948 and Dexter in 1953 [14,15], and has been well developed [16,17].

If Ce^* and Tb^* represent the Ce^{3+} and Tb^{3+} ions in their excited states, and Ce and Tb represent their ground states, respectively then the transition probability from $|Ce^*, Tb\rangle$to $|Ce, Tb^*\rangle$state, in accordance to the multipole interaction model, can be written as [18]

$$P_{Ce-Tb} = 2\pi/h|\langle Ce^*, Tb|H_{Ce-Tb}|Ce, Tb^*\rangle|^2 \int f_{Ce*}(E)\, f_{Tb}(E)\, dE, \quad (1)$$

where $H_{Ce-Tb}=(\frac{1}{4}\pi\varepsilon_0)(1/\kappa)\Sigma_{i,j}(e^2/|R+r_{Tbj}-r_{Cei}|)$ is the electrostatic interaction between electrons of Ce and Tb, and $f_{Ce*}(E)$and $f_{Tb}(E)$ are the normalized line-shape functions of the emission and excitation spectra of Ce^{3+} and Tb^{3+} respectively. The overlap of the normalized Ce^{3+} emission and Tb^{3+} excitation is quite well and much better than other host thus the energy transfer from the Ce^{3+} to Tb^{3+} could be very efficient. This could improve the excitation efficiency and brightness.

When Ce^{3+} concentration and Tb^{3+} concenration are equal to 1 mol%, the Ce^{3+}–Tb^{3+} spacing can be roughly taken as $R\approx 4.18$ nm together with the other parameters. We can estimate the rate of energy transfer through dipole–dipole interaction, P^{dd}_{Ce*Tb}, to be of about the order of $10^8\,s^{-1}$ [19]. The energy transfer through dipole–quadrupole interaction, $P^{dq}_{Ce*Tb}$is then of the order of $10^5\,s^{-1}$. The current concentrations of Ce^{3+} and Tb^{3+} are rather low, thus the system in this case is a diluted system. According to Eq. (1), P^{dd}_{Ce*Tb}will be increased to the order of $10^{10}\,s^{-1}$ and P^{dq}_{Ce*Tb}will be of the order of $10^7\,s^{-1}$ when the concentration of the dopants increases to 10%.

4. Conclusion

Luminescent materials, $CaAl_4O_7$:Ce^{3+}, $CaAl_4O_7$:Tb^{3+} and $CaAl_4O_7$:Tb^{3+}, Ce^{3+}, with emissions in the blue (440 nm) and in the green (545 nm) respectively, are synthesized. The samples show a pure single phase with monoclinic structure.

The broadband emission of $CaAl_4O_7$:Ce^{3+} at 440 nm includes the two transitions from 5d-excited state to the ground states $^2F_{5/2}$ and $^2F_{7/2}$. This luminescence feature certainly has an advantage for display techniques, which require a purer blue emission.

Strong green emission is observed and found to be greatly enhanced through an efficient energy transfer from Ce to Tb in $CaAl_4O_7$:Tb^{3+}, Ce^{3+}. It is estimated that about 95% of the total energy of the green emission of Tb^{3+} is transferred from Ce^{3+}. The energy transfer has a nature of dipole–dipole interaction with a rate approximately of the order of $10^8\,s^{-1}$.

The overlap of the Ce emission and Tb excitation line function is greatly improved because the Ce emission moves further to the lower energy side due to the new host ligands. Thus the energy transfer rate should be much higher. Because the energy transfer process in the Ce–Tb system is about 95%, the brightness and luminescent efficiency are better than other hosts. Thus $CaAl_4O_7$:Ce^{3+} and $CaAl_4O_7$:Tb^{3+}, Ce^{3+} must be interesting blue and green phosphors and may hold promise in applications to display devices.

Acknowledgements

National Natural Science Foundation of China supports this work.

References

[1] D. Jia, J. Zhu, B. Wu, J. Electrochem. Soc. 147 (1) (2000) 386.
[2] T.A. O'Brien, P.D. Rack, P.H. Holloway, M.C. Zerner, J. Lumin. 78 (1998) 245.
[3] D. Jia, B. Wu, J. Zhu, J. Lumin. 90 (2000) 33.
[4] D. Jia, J. Zhu, B. Wu, J. Lumin. 91 (2000) 59.
[5] L.G. Wisnyi, Acta Crystallogr. 11 (1958) 444.
[6] D.W. Goodwin, A.J. Lindop, Acta Crystallogr. B 26 (1970) 1230.
[7] A.M. Kevorkov, A.A. Kaminskii, Kh.S. Bagdasarov, T.A. Tevosyan, S.E. Sarkisov, Inorg. Mater. (USSR) 9 (1973) 146.

[8] H. Matsukiyo, H. Yamada, the 3rd International Conference on the Science and Technology of Disp. Phos., Extended Abstracts, 1997, p. 315.
[9] M.V. Hoffman, J. Electrochem. Soc. 118 (9) (1971) 1508.
[10] D. Jia, B. Wu, Y. Liu, J. Zhu, Advances in Materials Research & Application, C-MRS, Chemical Industrial Press, p. 371.
[11] B. Huttl, U. Troppenz, K.O. Velthaus, C.R. Ronda, R.H. Mauch, J. Appl. Phys. 78 (12) (1995) 7282.
[12] K.-S. Sohn, Y.Y. Choi, H.D. Park, Y.G. Choi, J. Electrochem. Soc. 147 (6) (2000) 2375.
[13] A. Mayolet, J.C. Krupa, J. SID 4/3 (1996) 173.
[14] Th. Forster, Ann. Phys. 2 (1948) 55.
[15] D.L. Dexter, J. Chem. Phys. 21 (5) (1953) 836.
[16] E. Nakazawa, Phosphor Handbook, in: S. Shionoya, W.M. Yen (Eds.), CRC Press, Boca Raton, Boston, London, New York, Washington, DC, 1999, p. 102.
[17] J.L. Sommerdijk, J.A.W. Van Der Dose De Bye, P.H.J.M. Verberne, J. Lumin. 14 (1976) 91.
[18] B. Henderson, G.F. Imbusch, Optical Spectroscopy of Inorganic Solids, Clarendon Press, Oxford, 1989, p. 445.
[19] K.-S. Sohn, Y.G. Choi, Y.Y. Choi, H.D. Park, J. Electrochem. Soc. 147 (9) (2000) 3352.